VERSITA

Cent. Eur. J. Chem. • 8(3) • 2010 • 646-651
DOI: 10.2478/s11532-010-0027-x

Central European Journal of **Chemistry**

A new zinc complex of 1-propyl-1H-benzo[*d*]imidazole: synthesis, characterization and electrocatalysis

Research Article

Rui Rui Zhuang, Fang Fang Jian*, KeFei Wang

New Materials & Function Coordination Chemistry Laboratory,
Qingdao University of Science and Technology,
Qingdao Shandong 266042, P.R. China

Received 21 October 2009; Accepted 8 January 2010

Abstract: The present work reports the synthesis, characterization and performance of a new zinc(II) complex of $[Zn(C_3H_7\text{-bim})_2Br_2]$ (bim = benzimidazole) as electrocatalyst for trichloroacetic acid and bromate reduction. Its structure was characterized by X-ray crystallography, IR spectroscopy and elemental analysis. The zinc atom adopts a distorted tetrahedral geometry by coordinating to two bromine atoms and two nitrogen atoms from two 1-propyl-1*H*-benzo[*d*]imidazole ligands. The electrochemical behavior and electrocatalysis of the zinc complex bulk-modified carbon paste electrode (Zn-CPE) have been studied by cyclic voltammetry. The Zn-CPE shows good electrocatalytic activities toward the reduction of trichloroacetic acid and bromate. The detection limit and the sensitivity are 0.05 μM, 67.43 μA μM^{-1} for trichloroacetic acid detection, and 0.02 μM, 69.94 μA μM^{-1} for bromate detection, respectively. This modified electrode shows good reproducibility, high stability, low detection limit, technical simplicity and possibility of rapid preparation, which is important for practical applications.

Keywords: *Zinc complex • Crystal structure • Electrocatalysis • Trichloroacetic acid • Bromate*

1. Introduction

The significant contemporary interest in organic-inorganic hybrid materials reflects both the fundamental chemistry of the rational design of complex materials and practical applications to fields as diverse as catalysis [1], optical materials [2-3], membranes [4-6] and sorption [7-8]. One synthetic strategy for design of inorganic-organic hybrid materials is to select suitable inorganic materials and organic ligands with the structure-directing properties [9-11]. In these hybrid materials, metal complexes with diverse structural arrangements not only serve as charge-compensating units but also modify the wide-ranging properties, such as magnetic and optical properties, electronic conductivities and electrocatalysis. Metal complexes are well recognized for their excellent electrocatalytic properties toward the detection of hydrogen peroxide [12-14], nitrite [12-15], bromate [13-15] and trichloroacetic acid [16] and so on. The electrochemistry and electrocatalysis of copper complexes with various different ligands have been investigated by several groups [14,15,17-19].

Interest in exploring benzimidazole derivatives and their metal complexes has continually increased, since many of these materials may serve as models which mimic both the structure and reactivity of metal ion sites in complex biological systems [20-27]. Sandoval *et al.* studied the synthesis, structure and biological activities of zinc(II) coordination compound with 2-benzimidazole derivatives [24]. Xu *et al.* investigated the structure diversity and anion exchange property of zinc(II) coordination polymers with flexible tripodal ligand 1,3,5-tris(imidazol-1-ylmethyl)benzene [25]. Aghatabay *et al.* reported the synthesis, characterization and antimicrobial activity of Zn(II) complex with 2,6-bis(benzimidazol-2-yl)pyridine ligand [26]. Guadarrama *et al.* studied the cytotoxic activity, X-ray crystal structures and spectroscopic characterization of cobalt(II), copper(II) and zinc(II) coordination compounds with 2-substituted benzimidazoles [27]. To the best of our knowledge, the study of the electrochemistry and electrocatalysis of zinc complexes containing benzimidazole are less reported [24-27]. The significance of this work is that it uses a new zinc complex $[Zn(C_3H_7\text{-bim})_2Br_2]$ as a bulk-modifier, to fabricate a chemically modified carbon paste electrode

---

* *E-mail: ffj2003@163169.net*

by direct mixing. This modified electrode shows good electrocatalytic activities towards the reduction of trichloroacetic acid and bromate.

2. Experimental Procedure

2.1. Chemicals and measurement

All the chemicals were of analytical reagent grade and used without further purification. Elemental analyses were measured with a Perkin-Elmer 1400C analyzer (USA). Infrared spectra was recorded on a Nicolet 170SX spectrometer (USA) using pressed KBr plates in the 4000–400 cm^{-1} ranges. Crystal structure determination by X-ray diffraction was performed on a Bruker-Nonius diffractometer with Kappa geometry with an attached APEXII-CCD detector (Bruker, Germany). Electrochemical measurements were performed by using an Autolab PGSTAT-30 digital potentiostat/galvanostat, (EcoChemie BV, Utrecht, Netherlands). A three-electrode cell was used in the experiments. The working electrode was modified CPE. The counter electrode was a platinum wire. The reference electrode was an Ag|AgCl, KCl(1 M)||, and all the potentials reported in this work were measured relative to this electrode (236.3 mV/SHE at 25°C). 0.1 M, pH 6.1 Britton-Robinson (B-R) buffer solution was used as the supporting electrolyte. All the solutions were de-aerated with pure nitrogen for 30 minutes and kept under nitrogen atmosphere during the experiments. All the measurements were performed at room temperature (25 ± 2°C).

2.2. Preparation and physical measurement of the zinc complex

Synthesis of $[Zn(C_3H_7\text{-bim})_2Br_2]$. Zinc bromide (225 mg, 1 mmol) and 1-propyl-1*H*-benzo[*d*]imidazole (320 mg, 2 mmol) were dissolved in ethanol solution (30 mL). After stirring for 2 h, the white precipitate was obtained by filtration. Recrystallization from acetonitrile gave a yield of 78%. The C, H and N contents were determined by elemental analysis (Anal. calcd for $C_{20}H_{24}Br_2N_4Zn$ (%) C 44.02, H 4.43, N 10.27; Found: C 44.05, H 4.45, N 10.23).

In the IR spectrum, the bands at 3057 and 750 cm^{-1} were assigned to the C–H(benzene ring) stretching vibration and bending vibration, respectively. The bands at 1611 and 1565 cm^{-1} were attributed to the vibration of benzene ring skeleton. The bands at 2953, 2876, 1465 and 1381 cm^{-1}, may be attributed to the C–H stretching vibration and bending vibration of the alkyl group. The band at 1238 cm^{-1} was attributed to the C–N stretching vibration of imidazole ring.

The crystal data collection has been carried out by CCD. X-ray diffraction was measured at 20°C using Mo K_α radiation (λ = 0.71073 Å) with a graphite monochromator. The structure of the zinc complex was solved by direct methods and refined by least squares on F_{obs}^2 by using the SHELXTL software package [28]. All nonhydrogen atoms were refined anisotropically, and the hydrogen atoms were placed in the calculated position and allowed to ride on their parent atoms. The molecular graphics was plotted using the SHELXTL. Atomic scattering factors and anomalous dispersion corrections were taken from the International Tables for X-ray Crystallography [29].

2.3. Preparation of Zn-CPE

The traditional carbon paste electrode (CPE) was prepared by hand-mixing of graphite powder with paraffin oil at a ratio of 70:30 (w/w) in an agate mortar. The zinc complex was employed to fabricate modified carbon paste electrodes due to its insolubility in water and Britton-Robinson buffer solution (pH 6.1). The modified CPE was fabricated as follows: 0.3 g of graphite powder and 0.03 g of the zinc complex were mixed and ground together using agate mortar and pestled for about 30 minutes to achieve an even, dry mixture. Paraffin oil (0.1 mL) was added to the mixture and stirred with a glass rod. A portion of the carbon paste was filled firmly into one end of a glass tube (3 mm inner diameter), and a copper wire was inserted through the opposite end to establish an electrical contact. The surface of the Zn-CPE was polished with smooth tissue until it had a metallic shine and showed good mechanical strength.

The different quality ratios of graphite powder and the zinc complex were investigated to determine the optimum preparation condition. We investigated the graphite powder and the zinc complex at the ratios of 20:1, 14:1, 10:1, 8:1 and 5:1 (w/w), and found that the optimum preparation condition was 10:1. When the amount of the zinc complex was too low, the electrochemical signal was weak. Conversely, when the amount of the zinc complex was high, the conductivity of the modified carbon paste electrode was low.

3. Results and discussion

3.1. Crystal structure of the zinc complex

The molecular structure of $[Zn(C_3H_7\text{-bim})_2Br_2]$ with the atomic numbering scheme is shown in Fig. 1. Crystal data and structure refinement are listed in Table 1. The zinc atom adopts a distorted tetrahedral geometry by coordinating to two bromine atoms and two nitrogen atoms from two 1-propyl-1*H*-benzo[*d*]imidazole ligands. The entire complex is highly non-symmetrical both in the bromine ligands and the benzimidazole ligands. The dihedral angles between the two benzimidazole rings to the plane [Zn–Br(1)–Br(2)] are 22.69° and 69.44°,

Table 1. Crystal data and structure refinement for [Zn(C_3H_7-bim)$_2$Br$_2$]

Empirical formula	$C_{20}H_{24}Br_2N_4Zn$
Formula weight	545.62
Temperature (K)	293(2)
Wavelength (Å)	0.71073
Crystal system, space group	Monoclinic, $P2_1/c$
Unit cell dimensions	
a (Å)	10.081(5)
b (Å)	14.289(5)
c (Å)	15.831(5)
α(°)	90
β (°)	95.341(5)
γ (°)	90
Volume (Å^3)	2270.5(16)
Z, Calculated density (g cm^{-3})	4, 1.596
Absorption coefficient (mm^{-1})	4.613
F(000)	1088
Theta range for data collection (°)	3.13 to 27.48
Limiting indices	$-13 \le h \le 13$, $-18 \le k \le 18$, $-19 \le l \le 20$
Reflections collected / unique	21930 / 5200 [$R_{(int)} = 0.0844$]
Completeness to θ = 27.48 (%)	99.8
Data / restraints / parameters	5200 / 0 / 246
Goodness-of-fit on F^2	1.075
Final R indices [I > 2σ(I)]	$R_1 = 0.0955$, $wR_2 = 0.2803$
R indices (all data)	$R_1 = 0.1644$, $wR_2 = 0.3439$
Largest diff. peak and hole (e Å^{-3})	1.299 and –1.489

respectively. There are also some minor differences in band lengths and bond angles around Zn atom. The Zn–N bonds distances [Zn(1)–N(4) 2.000(8) Å, Zn(1)–N(2) 2.011(9) Å] and Zn–Br bonds distances [Zn(1)–Br(2) 2.385(2)Å and Zn(1)–Br(1) 2.413(2) Å] are comparable with those found in the similar structures reported earlier [25,27]. The angles around the Zn center [N(4)–Zn(1)–N(2) 101.9(3)°, N(4)–Zn(1)–Br(2) 111.9(2)°, N(2)–Zn(1)–Br(2) 114.8(2)°, N(4)–Zn(1)–Br(1) 109.6(2)°, N(2)–Zn(1)–Br(1) 105.8(2)°, Br(2)–Zn(1)–Br(1) 112.31(7)°] are consistent with the similar structures reported earlier [25,27]. There is weak potentially intermolecular C–H···N hydrogen bond interaction, with the donor-acceptor distance of 3.0882 Å for C(11A)···N(1). The other feature of intermolecular interaction is due to one type of C–H···*π* supramolecular interaction. The distance between C(11A)–H(11A) to the plane [N(1)–N(2)–C(4)–C(9)–C(10)] is 3.325Å. In the solid state, the intermolecular interactions in this structure stabilize the crystal structure.

3.2. Electrochemical behavior of Zn-CPE

The electrochemical behavior of the Zn-CPE was investigated by cyclic voltammetry in the aqueous solution. We chose a 0.1 M KCl aqueous solution, 0.1 M, pH 7.0, Britton-Robinson (B-R) buffer solution and 0.1 M, pH 7.0, phosphate buffer solution as the supporting electrolyte solutions. It was found that the modified electrode in B-R buffer solution showed strong current response and symmetric peak shape. Then, we investigated the electrochemical behavior of modified CPE in the pH range from 4.0 to 8.0 B-R buffer solution and found that the electrochemical signal was relatively stable at pH 6.1. Therefore, we studied the electrochemical behavior and electrocatalytic properties in 0.1 M, pH 6.1, B-R buffer solution.

The cyclic voltammograms (CVs) of Zn-CPE are presented in Fig. 2. In the potential range 0 to –1.5 V, there was no redox peak at the bare CPE. While at

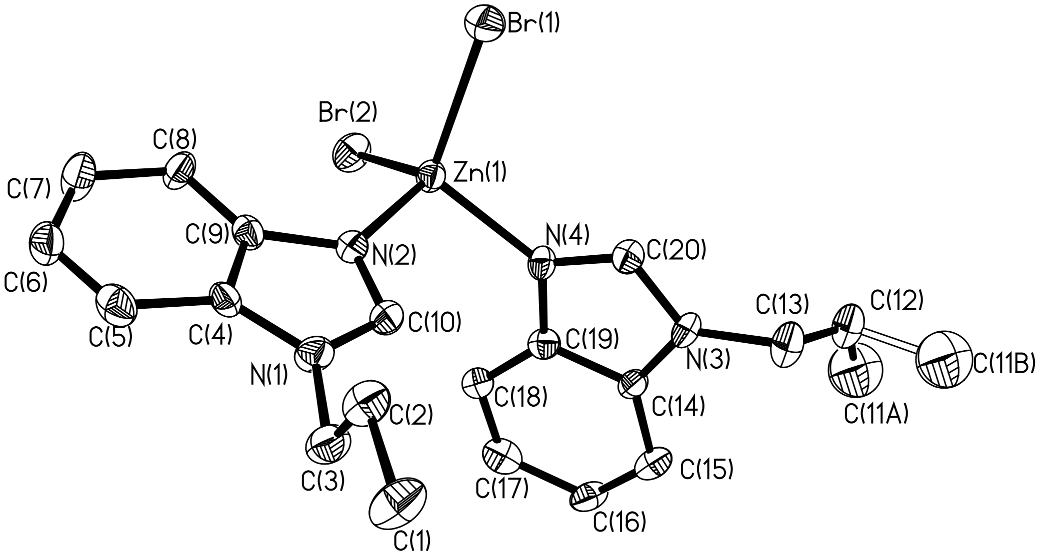

Figure 1. The molecular structure of [Zn(C_3H_7-bim)$_2$Br$_2$] with the atomic numbering scheme.

the modified Zn-CPE, the curve **a** had a couple of well-defined redox peaks at –0.819 V and –0.688 V, with the formal potential ($E^{0'}$) at –0.753 V, corresponding to the electrochemical process of Zn(II)/Zn(I). The separation of the cathodic and anodic peak potential, $\Delta E = 0.131$ V, $i_{pc}/i_{pa} = 1.06$, indicating that the electrochemical behavior of the zinc complex on the electrode was quasi-reversible.

The effect of scan rate on the electrochemical behavior of the Zn-CPE can be seen from Fig. 2. When the scan rate was varied from 0.03 to 0.30 V s^{-1}, the peak potentials changed gradually: the cathodic peak potentials shifted to the negative direction and the corresponding anodic peak potentials shifted to the positive direction with increasing scan rate. The plot of peak current *versus* scan rate is shown in the inset of Fig. 2. The anodic and cathodic currents are proportional to the scan rates, suggesting that the redox process is confined to the surface.

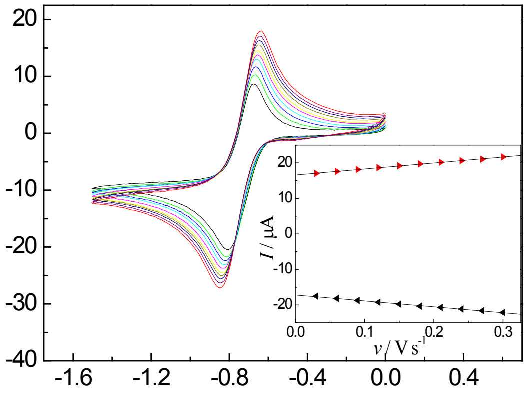

Figure 2. CVs of Zn-CPE in 0.1 M, pH 6.1, B-R buffer solution. Curves (a–j) correspond to the scan rates 0.03, 0.06, 0.09, 0.12, 0.15, 0.18, 0.21, 0.24, 0.27 and 0.30 V s^{-1}, respectively. Inset: the peak current versus scan rate.

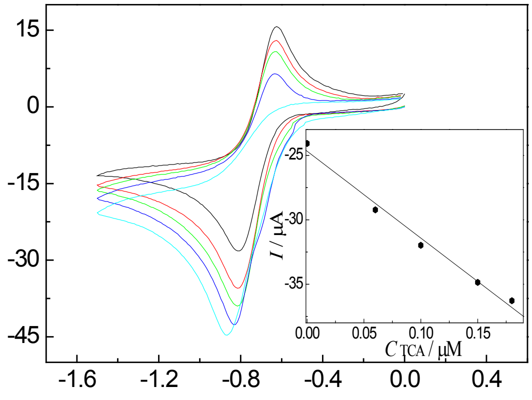

Figure 3. CVs of Zn-CPE in 0.1 M, pH 6.1, B-R buffer solution containing (a–e) 0, 0.06, 0.10, 0.15 and 0.18 μM TCA with the scan rate as 0.15 V s^{-1}. Inset: the cathodic peak current versus TCA concentration.

3.3. Electrocatalytic activity of the Zn-CPE

3.3.1. Electrocatalytic reduction of trichloroacetic acid (TCA)

TCA is an environmental pollutant forms during water chlorination. Electrochemical oxidation or reduction is a kind of effective measure to deal with pollutants of environment [16]. The electrocatalytic activity towards TCA of Zn-CPE is shown in Fig. 3. With the addition of TCA to the solution (curves **a**–**e**), there was little change in the oxidation and reduction peak potentials, but there was a dramatic enhancement of the cathodic peak current and the anodic peak current decreased. When the concentration of TCA was increased to 0.18 μM, the maximum value of the reduction peak current was obtained, while the value of the oxidation peak current was almost reduced to zero, which indicated a strong catalytic effect. The possible reaction processes have been discussed in some references [16,30].

The inset of Fig. 3 shows that the catalytic current is linear *versus* TCA concentration in the range of 0.06–0.18 μM. The linear regression equation is $I_{pc}(\mu A) = -67.43C(\mu M) - 24.68$ with a correlation coefficient of 0.993. The detection limit (signal to noise is 3) and the sensitivities are 0.05 μM and 67.43 μA μM^{-1}, respectively.

3.3.2. Electrocatalytic reduction of bromate

The overpotential for bromate reduction is high and therefore an efficient electrocatalyst would be beneficial [14,30-32]. The reduction of bromate can readily be catalyzed by Zn-CPE in 0.1 M, pH 6.1, B-R buffer solution. As shown curves **a**–**e** in Fig. 4, with the addition of bromate, the peak potentials had little change, and the reduction peak currents increased while the corresponding oxidation peak decreased. When the concentration of bromate was increased to 0.20 μM, the maximum value of the reduction peak current was obtained, while the value of the oxidation peak current was almost reduced to zero, indicating that Zn-CPE had excellent electrocatalytic activity towards the reduction of bromate. The possible reaction processes has been discussed in some references [14,30].

The inset of Fig. 4 shows that the catalytic current varies linearly with bromate concentration in the range of 0.05–0.20 μM. The linear regression equation is $I_{pc}(\mu A) = -69.94C(\mu M) - 19.68$ with a correlation coefficient of 0.996. The detection limit (signal to noise is 3) and the sensitivity are 0.02 μM and 69.94 μA μM^{-1}, respectively. Comparison of performances of different

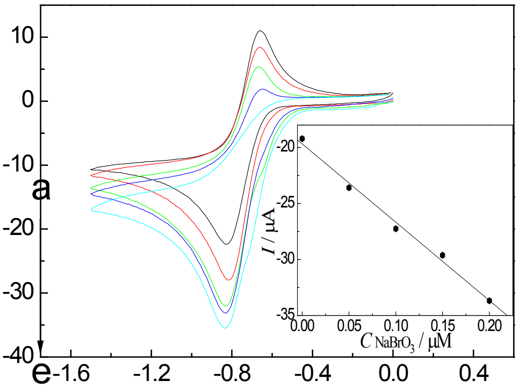

Figure 4. CVs of Zn-CPE in 0.1 M, pH 6.1, B-R buffer solution containing (a–e) 0, 0.05, 0.10, 0.15 and 0.20 μM bromate with the scan rate as 0.15 V s^{-1}. Inset: the cathodic peak current versus bromate concentration.

electrochemical sensors for bromate, reveal that this detection limit is much lower than earlier reports (0.1 μM [17], 0.036 μM [31] and 0.6 μM [32]) in which other modified electrodes were used.

Compared with other modified film electrodes, the zinc complex modified electrode showed high stability. In our experiment, after the electrocatalytic reaction, the Zn-CPE was investigated in buffer solution under the same conditions as shown in Fig. 2, we found that there was little difference in the peak potentials and peak currents, which suggested that no new materials appeared. This indicated that the zinc complex was still stable and played the role of a catalyst during the reactions. When the potential range was maintained at the same range, it was stable over 100 cycles at a scan rate of 0.15 V s^{-1} and the current response remained almost unchanged. When Zn-CPE was stored at room temperature for at least two month the current response decreased only by 2.6%.

4. Conclusions

In summary, a new complex of [Zn(C_3H_7-bim)$_2$Br$_2$] was synthesized and its structure was characterized. The electrochemical behavior and electrocatalysis of the Zn-CPE was investigated. This modified electrode shows excellent electrocatalytic activities toward the reduction of trichloroacetic acid and bromate. The detection limit and the sensitivity are 0.05 μM, 67.43 μA μM^{-1} for trichloroacetic acid detection, and 0.02 μM, 69.94 μA μM^{-1} for bromate detection. Comparison of performances of different electrochemical sensors for bromate, showed that the detection limit in this study is much lower than earlier reports (0.1 μM [17], 0.036 μM [31] and 0.6 μM [32]) in which other modified electrodes were used, and hence may be suitable for the quantitive analysis of environmentally hazardous materials. The advantages of the bulk-modified Zn-CPE are stability, good catalytic activity, low detection limit and simplicity of preparation. These preliminary results in this work represent potential applications on electrochemical sensors

Acknowledgement

This work was supported by the Natural Science Foundation of Shandong Province (No.Z2007B01), P. R. China.

Supplementary material

Crystallographic data of the structural analysis have been deposited at the Cambridge Crystallographic Data Centre, CCDC reference number 750009. Copies of this information can be obtained free of charge from The Director, 12 Union Road, Cambridge, CB2 1EZ, UK (fax: +44-1223-336033; e-mail: deposit@ccdc.cam.ac.uk or http://www.ccdc.cam.ac.uk).

References

[1] H.L. Ngo, A.G. Hu, W.B. Lin, J. Mol. Catal. A 215, 177 (2004)
[2] O.R. Evans, W.B. Lin, Chem. Mater. 13, 3009 (2001)
[3] C. Sanchez, B. Lebeau, F. Chaput, J.P. Boilet, Adv. Mater. 15, 1969 (2003)
[4] I. Honma, S. Nomura, H. Nakajima, J. Membr. Sci. 185, 83 (2001)
[5] A. Javaid, M.P. Hughey, V. Varutbangkul, D.M. Ford, J. Membr. Sci. 187, 141 (2001)
[6] P. Jannasch, Curr. Opin. Colloid Interface Sci. 8, 96 (2003)
[7] A.C. Sudik, A.R. Millward, N.W. Ockwig, A.P. Cote, J. Kim, O.M. Yaghi, J. Am. Chem. Soc. 127, 7110 (2005)
[8] J.L.C. Rowsell, A.R. Millward, K.S. Park, O.M. Yaghi, J. Am. Chem. Soc. 126, 5666 (2004)
[9] Z. Takáts, J.M. Wiseman, B. Gologan, R.G. Cooks, Anal. Chem. 76, 4050 (2004)
[10] S. Liu, D.G. Kurth, D. Volkmer, Chem. Commun. 976 (2002)
[11] F. Lisdat, R. Dronov, H. Möhwald, F.W. Scheller,

D.G. Kurthw, Chem. Commun. 274 (2009)

[12] X.L. Wang, Z.H. Kang, E.B. Wang, C.W. Hu, J. Electroanal. Chem. 523, 142 (2002)

[13] X.L. Wang, E.B. Wang, Y. Lan, C.H. Hu, Electroanalysis 14, 1116 (2002)

[14] X.L. Wang, H.Y. Zhao, H.Y. Lin, G.C. Liu, J.N. Fang, B.K. Chen, Electroanalysis 20, 1055 (2008)

[15] X.L. Wang, H.Y. Lin, G.C. Liu, H.Y. Zhao, B.K. Chen, J. Organomet. Chem. 693, 2767 (2008)

[16] X.E. Jiang, L.P. Guo, X.G. Du, Talanta 61, 247 (2003)

[17] A. Salimi, V. Alizadeh, H. Hadadzadeh, Electroanalysis 16, 1984 (2004)

[18] S.M. Chen, J. Electroanal. Chem. 457, 23 (1998)

[19] R.R. Zhuang, F.F. Jian, K.F. Wang, Sci. Technol. Adv. Mater. 10, 045001 (2009)

[20] J.D. Crane, E. Sinn, B. Tann, Polyhedron 18, 1527 (1999)

[21] Z. Liu, Y. Chen, P. Liu, J. Wang, M.H. Huang, J. Solid State Chem. 178, 2306 (2005)

[22] C.K. Xia et al., J. Mol. Struct. 831, 195 (2007)

[23] F. Arjmand, M. Aziz, Eur. J. Med. Chem. 44, 834 (2009)

[24] H. López-Sandoval et al., J. Inorg. Biochem. 102, 1267 (2008)

[25] G.C. Xu, Y.J. Ding, Y.Q. Huang, G.X. Liu, W.Y. Sun, Microporous Mesoporous Mater. 113, 511 (2008)

[26] N.M. Aghatabay, A. Neshat, T. Karabiyik, M. Somer, D. Haciu, B. Dülger, Eur. J. Med. Chem. 42, 205 (2007)

[27] O. Sánchez-Guadarrama, H. López-Sandoval, F. Sánchez-Bartéz, I. Gracia-Mora, H. Höpfl, N. Barba-Behrens, J. Inorg. Biochem. 103, 1204 (2009)

[28] G.M. Sheldrick, SHELXTL, Version 6.10. (Bruker AXS Inc., Madison, Wisconsin, USA, 2000)

[29] A.J. Wilson, International table for X-ray crystallography (Kluwer Academic Publishers, Dordrecht, 1992) 500

[30] Y.X. Li, X.Q. Lin, C.M. Jiang, Electroanalysis 18, 2085 (2006)

[31] A. Salimi, B. Kavosi, A. Babaei, R. Hallaj, Anal. Chim. Acta 618, 43 (2008)

[32] A. Salimi, H. Mamkhezri, R. Hallaj, S. Zandi, Electrochim. Acta 52, 6097 (2007)